Materials Letters 292 (2021) 129635

Contents lists available at ScienceDirect

Materials Letters

journal homepage: www.elsevier.com/locate/mlblue

Facile synthesis of ZnO/ZnS heterojunction nanoarrays for enhanced piezo-photocatalytic performance

Zeqian Ren [a], Xiu Li [a], Lixia Guo [a], Jizhou Wu [a,b], Yuqing Li [a,b], Wenliang Liu [a,b], Peng Li [a], Yongming Fu [a,*], Jie Ma [a,b,*]

[a] School of Physics and Electronic Engineering, Institute of Laser Spectroscopy, State Key Laboratory of Quantum Optics and Quantum Optics Devices, Shanxi University, Taiyuan 030006, China
[b] Collaborative Innovation Center of Extreme Optics, Shanxi University, Taiyuan 030006, China

ARTICLE INFO

Article history:
Received 22 January 2021
Received in revised form 27 February 2021
Accepted 1 March 2021
Available online 7 March 2021

Keywords:
Nanocomposites
Piezoelectric materials
Energy storage and conversion

ABSTRACT

Constructing heterojunction is a promising approach to enhance the piezo-photocatalytic performance of ZnO nanostructures. In this study, ZnO/ZnS heterojunction nanoarrays have been synthesized by facile vulcanizing surface of wurtzite ZnO nanorods into blende ZnS nanoparticles through hydrothermal method. Both the synthesized wurtzite ZnO nanorods and blende ZnS nanoparticles are piezoelectric semiconductors with wide band gaps. For degrading methyl blue solution under UV irradiation and ultrasonic sonication, it is found that both the piezocatalytic, photocatalytic and piezo-photocatalytic performances of ZnO/ZnS nanoarrays are much higher than those of pure ZnO. In addition, the piezo-photocatalytic degradation rate of ZnO/ZnS nanoarrays can be further increased by improving the ultrasonic power. The mechanism can be attributed to the synergetic effect of piezoelectric effect and heterojunction photocatalysis.

1. Introduction

The growing awareness of water protection has attracted worldwide attentions for developing novel pollution treatment methods. Among the green techniques for wastewater treatment, photocatalysis based on semiconductor nanomaterials has been considered as the most promising candidate by utilizing solar energy to degrade organic pollutants into non-toxic inorganics [1–3]. Generally, the recombination of photogenerated charge carriers essentially restrains the photocatalytic degradation performance of nanostructured photocatalysts, which can be improved by applying external electric field, constructing heterojunction, decorating noble metal, etc [4–6]. For example, the complex iron oxides with excellent electronic properties have been synthesized for improving photocatalytic performances [7,8]. However, the expensive costs and harsh conditions restrict the applications of these photocatalytic techniques.

In recent years, the concept of piezoelectric photocatalysis with high performance has been realized by bending ZnO nanowires to generate piezoelectric field to drive more electrons migrating to nanowire/solution interface and triggering redox reactions [9–11]. Various stress-sensitive nanomaterials available for piezo-photocatalysis have been developed, such as ZnO, CdS and $BaTiO_3$, whereas the separation efficiency of photogenerated charge carriers is inhibited by the nature of individual nanomaterials [12–14]. With further investigation of piezo-photocatalysis, the architecture of composite piezo-photocatalysts may be an effective approach to enhance the charge separation since the combination of different compounds which have excellent electronic properties can significantly improve the electronic properties [15,16]. Moreover, developing a facile approach for constructing heterojunction using two kinds of nanomaterials with appropriate band structure is also necessary [17,18].

In this study, ZnO/ZnS heterojunction nanoarrays have been synthesized to enhance piezo-photocatalytic performance by facile sulfidation of ZnO nanorods through hydrothermal method. Both the wurtzite ZnO nanorods and blende ZnS nanoparticles are piezoelectric n-type semiconductors for UV absorption. The impact of piezoelectric on the photocatalysis of ZnO/ZnS nanoarrays has been investigated by sonication assistant photocatalytic degradation of organic pollutant, suggesting that piezoelectric can enhance the heterojunction photocatalysis of ZnO/ZnS nanoarrays.

* Corresponding authors at: School of Physics and Electronic Engineering, Institute of Laser Spectroscopy, State Key Laboratory of Quantum Optics and Quantum Optics Devices, Shanxi University, Taiyuan 030006, China (J. Ma).
E-mail addresses: fuyongming@sxu.edu.cn (Y. Fu), mj@sxu.edu.cn (J. Ma).

https://doi.org/10.1016/j.matlet.2021.129635
0167-577X/

2. Experimental

ZnO/ZnS nanoarrays were synthesized on Ni foam substrate through hydrothermal method. Typically, a piece of commercial Ni foam was ultrasonically cleaned in water/alcohol for 20 min and dried at 60 °C. Then, 2.5 mL ammonium hydroxide was added into 47.5 mL $ZnNO_3$ aqueous solution (0.05 M) drop by drop. After stirring for 10 min, the cleaned Ni foam was immersed into the above solution, sealed and heated at 80 °C for 10 h to grow ZnO nanorod arrays on Ni foam. To obtain ZnO/ZnS heterojunction, the ZnO-coated Ni foam was sulfureted by immersing into 50 mL thioacetamide aqueous solution (0.02 M) at 200 °C for 24 h.

The morphology, component element, optical property and microstructure were conducted by scanning electron microscopy (SEM), energy dispersive spectroscopy (EDS), X-ray diffractometer (XRD), UV–Vis diffuse reflection spectrum (DRS) and transmission electron microscopy (TEM).

The piezo-photocatalytic performance of ZnO/ZnS heterojunction was analyzed qualitatively by degrading methylene blue (MB, 5 mg/L) under ultrasonic sonication (US) and UV irradiation. Before degradation, the as-grown Ni foam was immersed into 50 mL MB solution in dark for 30 min to achieve adsorption–desorption equilibrium. 2 mL MB solution was taken out every 10 min to measure MB concentration by spectrophotometer. The degradation rate is calculated by subtracting a ratio from a hundred percent, where the ratio is recorded from the peak intensity located at 665 nm between the initial (C_0) and treated (C) solution.

3. Results and discussion

ZnO nanoarrays are grown on porous Ni foam to generate large piezoelectricity and reduce the mass loss during re-use process. Fig. 1a is the SEM image of ZnO/ZnS nanoarrays, indicating that ZnO nanorods are vertically grown on Ni foam along the same orientation and evenly wrapped with ZnS nanoparticles. Fig. 1b is the EDS spectrum, indicating the existence of O, Zn, S and Ni element. Ni element is derived from the Ni foam substrate and S element corroborates the sulfidation process for the formation of ZnS. Fig. 1c shows the XRD pattern of ZnO/ZnS nanorod arrays. The peaks marked by pound sign and asterisk are dependent to blende ZnS (PDF card No. 05-0566) and hexagonal wurtzite ZnO (PDF card No. 36-1451), respectively [19]. Fig. 1d is the DRS spectra of pure ZnO and ZnO/ZnS nanorod arrays, displaying the absorption threshold lower than 400 nm. For ZnO/ZnS, there are two strong UV absorption peaks located at ~371 and 324 nm, which can be attributed to the electronic transition of ZnO and ZnS, respectively [20].

Fig. 2a is the TEM image of single ZnO/ZnS nanorod. The heterojunction remains one-dimensional morphology with diameter of ~400 nm and length of ~3 μm after sulfidation process. Fig. 2b is the magnified TEM image, further showing that ZnO nanorod is tightly covered with ZnS nanoparticles. Fig. 2c is the high-resolution TEM image, describing the interface of ZnO/ZnS heterojunction with high crystallinity. The distances of marked lattice fringes are 0.26 and 0.31 nm, corresponding to the (002) lattice plane of hexagonal wurtzite ZnO and the (111) lattice plane of blende ZnS, respectively. Fig. 2d is the selected area electron diffraction (SAED) pattern of ZnO/ZnS heterojunction. Three discrete diffraction rings can be observed according to (111), (220) and (311) lattice planes of blende ZnS. It is noting that no obvious ZnO diffraction lattices can be observed, further confirming the ZnS nanoparticle shell tightly covering on ZnO nanorods.

Fig. 3 shows the degradation rates of MB catalyzed by pure ZnO and ZnO/ZnS nanoarrays under different conditions. Under 300 W UV irradiation, 180 W sonication and both, the degradation rates of pure ZnO are 11.6%, 26.4% and 39.9% (Fig. 3a), while those of ZnO/ZnS increase to 19.1%, 32.2% and 53.8%, respectively (Fig. 3b). These results reveal that both the piezocatalytic, photocatalytic and piezo-photocatalytic properties of ZnO/ZnS are higher than that of pure ZnO, which can be attributed to the formation of ZnO/ZnS heterojunction. With the ultrasonic power increases from

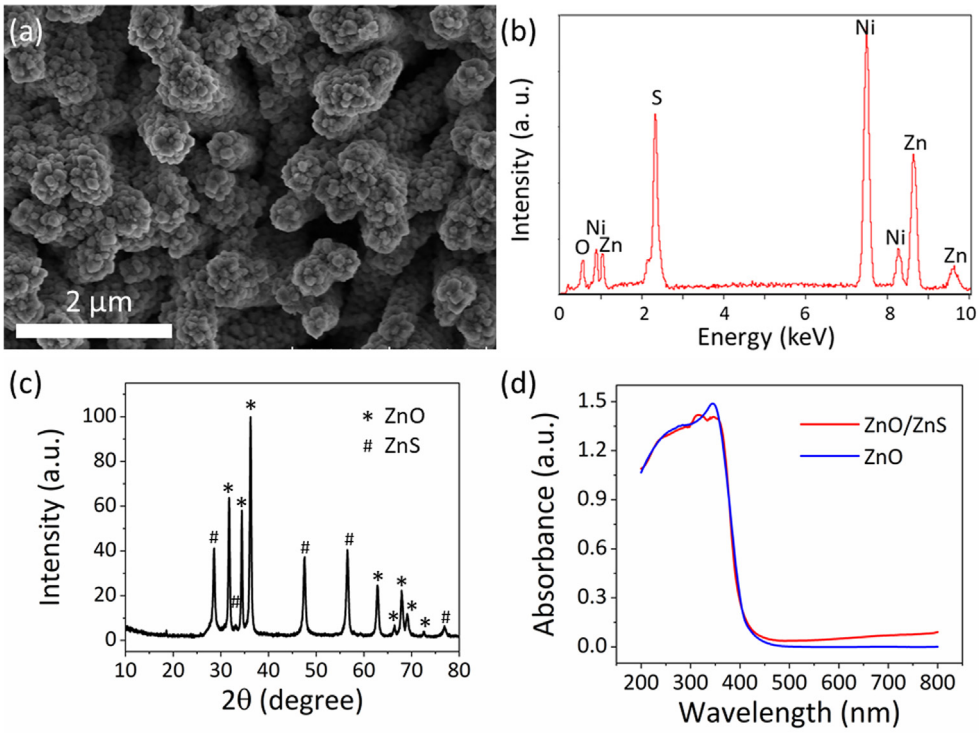

Fig. 1. (a) SEM image of ZnO/ZnS nanoarrays. (b) EDS spectrum. (c) XRD pattern. (d) DRS spectra.

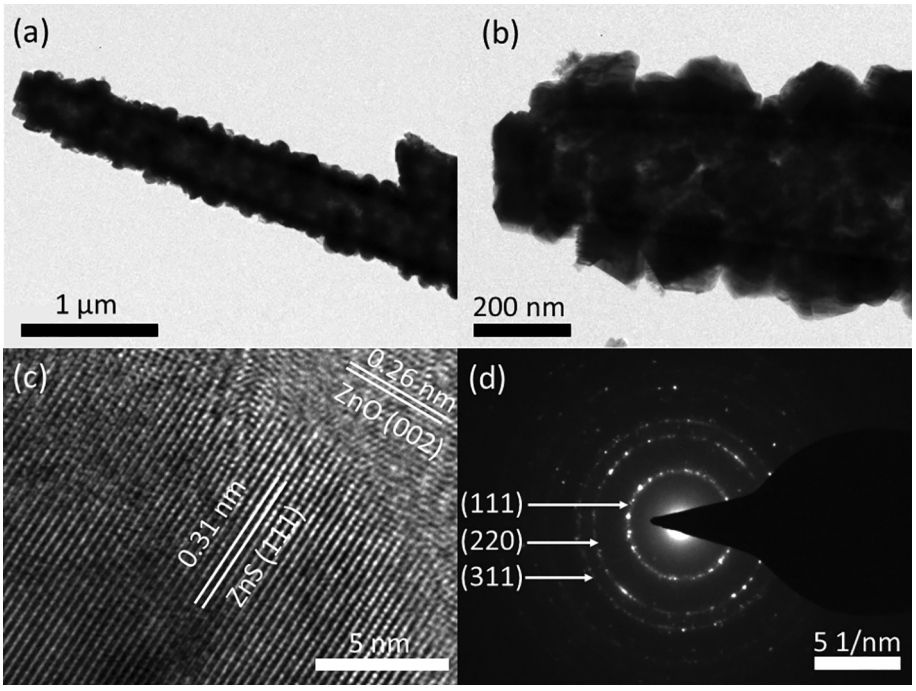

Fig. 2. (a) TEM image. (b) Magnified image. (c) High-resolution TEM. (d) SAED pattern.

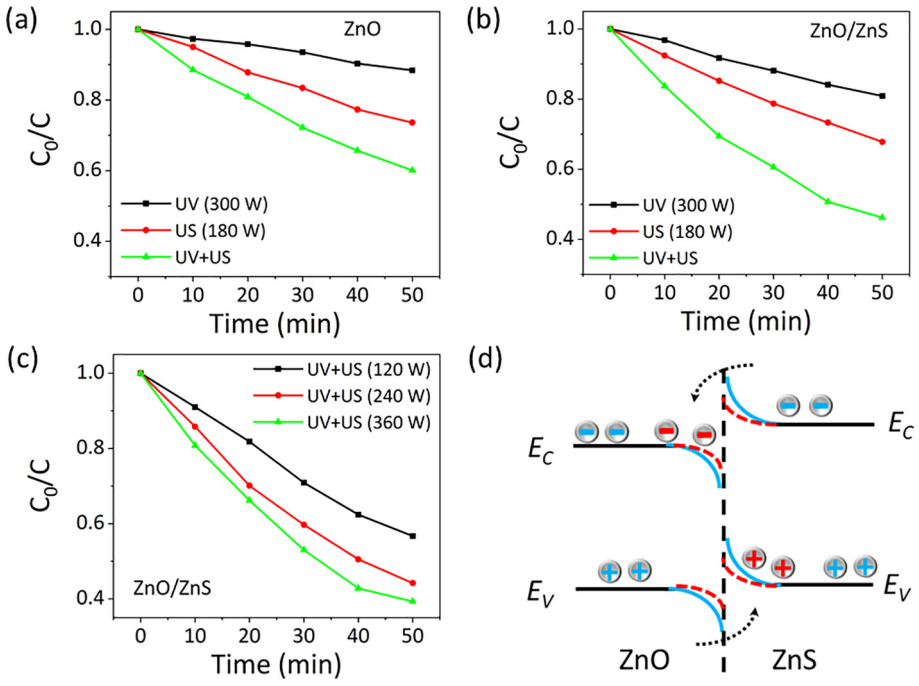

Fig. 3. (a–c) The degradation rates under different conditions of (a) pure ZnO, (b) ZnO/ZnS heterojunction and (c) increasing ultrasonic power. (d) Mechanism diagram.

120 to 360 W, the piezo-photocatalytic degradation rate of ZnO/ZnS increases from 43.3% to 60.7%, owing to the synergetic effect of piezo-photocatalysis and heterojunction (Fig. 3c).

The mechanism of piezoelectric promoted photocatalytic degradation can be diagramed in Fig. 3d. Previous literatures have reported that the addition of a second phase can significantly improve the electronic properties of the resulting composite material by coupling the excellent electronic properties of two components [15,16]. In this case, ZnO and ZnS can form heterojunction and the band offset occurs to re-balance Fermi energy level [21]. Upon exposure to UV irradiation, the electrons in valence band can be excited to conduction band for forming free electrons and leaving holes in valence band, accompanied with recombination of electron-hole pairs simultaneously. Then, the free electrons migrate from conductor band of ZnS to ZnO, while the holes will migrate along opposite direction and accumulate at valence band of ZnS, which can spatially separate and inhibit the recombination of electron-hole pairs (blue solid lines). The separated electrons and holes can migrate to semiconductor/solution interface, react with hydroxyl and superoxide ions, generate reactive oxygen

species and finally degrade MB molecules, realizing heterojunction photocatalysis. Under ultrasonic sonication, the piezoelectric field with opposite direction can be established in ZnO and ZnS to decrease the energy barriers. Thus, more free electrons and holes can pass through the interface, resulting in higher spatial separation to further hinder the recombination of electron-hole pairs (red dash line). Thus, the photocatalytic degradation rate is enhanced.

4. Conclusions

In summary, ZnO/ZnS nanorod arrays have been synthesized through facile hydrothermal method to enhance the piezo-photocatalytic degradation performance. Both the piezocatalytic, photocatalytic and piezo-photocatalytic performances of ZnO/ZnS nanoarrays are much higher than pure ZnO nanoarrays. In addition, the piezo-photocatalysis of ZnO/ZnS nanoarrays increase with increasing piezoelectricity induced by ultrasonic sonication. The enhancement of piezo-photocatalysis can be attributed to the inhibited combination and increased spatial separation of photo-generated electron-hole pairs by synergetic effect of piezoelectricity and heterojunction photocatalysis. This work expands the sight of piezotronics and provides a promising approach for enhancing the photocatalytic performance.

CRediT authorship contribution statement

Zeqian Ren: Resources, Investigation. **Xiu Li:** Investigation. **Lixia Guo:** Visualization. **Jizhou Wu:** Writing - original draft. **Yuqing Li:** Methodology. **Wenliang Liu:** Writing - review & editing. **Peng Li:** Visualization. **Yongming Fu:** Conceptualization, Investigation, Writing - original draft. **Jie Ma:** Writing - review & editing, Supervision, Project administration.

Declaration of Competing Interest

The authors declare that they have no known competing financial interests or personal relationships that could have appeared to influence the work reported in this paper.

Acknowledgements

This work was supported by the National Key Research and Development Program of China (No. 2017YFA0304203), the National Natural Science Foundation of China (No. 61722507, 61675121, 61705123, 61901249 and 62020106014), PCSIRT (No. IRT_17R70), 111 project (No. D18001), the Innovation Project of Graduate Education in Shanxi (No. 2020SY058), Scientific and Technological Innovation Programs of Higher Education Institutions in Shanxi (No. 2019L0002), the Program for the Outstanding Innovative Teams of Higher Learning Institutions of Shanxi (OIT), the Applied Basic Research Project of Shanxi Province (No. 201801D221004, 201901D211191 and 201901D211188), the Shanxi 1331 KSC and collaborative grant by the Russian Foundation for Basic Research and NSF of China (No. 62011530047 and 20-53-53025 in the RFBR classification).

References

[1] X. Li, J. Yu, M. Jaroniec, Chem. Soc. Rev. 45 (2016) 2603–2636.
[2] M. Liras, M. Barawi, V.A.d.l.P. O'Shea, Chem. Soc. Rev. 48 (2019) 5454–5487.
[3] P. Zhou, J. Yu, M. Jaroniec, Adv. Mater. 26 (2014) 4920–4935.
[4] A. Dhakshinamoorth, A.M. Asiri, H. Garcia, Adv. Mater. 31 (2019) 1900617.
[5] X. Liu, J. Iocozzia, Y. Wang, et al., Energy Environ. Sci. 10 (2017) 402–434.
[6] J. Low, J. Yu, M. Jaroniec, et al., Adv. Mater. 29 (2017) 1601694.
[7] S.V. Trukhanov, A.V. Trukhanov, V.G. Kostishyn, et al., J. Magn. Magn. Mater. 426 (2017) 554–562.
[8] A.L. Kozlovskiy, I.E. Kenzhina, M.V. Zdorovets, Ceram. Int. 46 (2020) 10262–10269.
[9] H. Li, Y. Sang, S. Chang, et al., Nano Lett. 15 (2015) 2372–2379.
[10] Z. Liang, C.-F. Yan, S. Rtimi, et al., Appl. Catal. B Environ. 241 (2019) 256–269.
[11] X. Xue, W. Zang, P. Deng, et al., Nano Energy 13 (2015) 414–422.
[12] N. Hao, Z. Xu, Y. Nie, et al., Chem. Eng. J. 378 (2019) 122222.
[13] S. Xu, L. Guo, Q. Sun, et al., Adv. Funct. Mater. 29 (2019) 1808737.
[14] Y. Zhao, X. Huang, F. Gao, et al., Nanoscale 11 (2019) 9085–9090.
[15] M.M. Salem, L.V. Panina, E.L. Trukhanova, et al., Compos. B: Eng. 174 (2019) 107054–107058.
[16] A.L. Kozlovskiy, M.V. Zdorovets, Compos. B: Eng. 191 (2020) 107968.
[17] M.A. Almessierea, Y. Slimania, A.V. Trukhanov, et al., J. Ind. Eng. Chem. 90 (2020) 251–259.
[18] M.V. Zdorovets, A.L. Kozlovskiy, J. Alloys Compd. 815 (2020) 152450.
[19] R. Zhang, J. Xie, C. Wang, et al., J. Mater. Sci. 52 (2017) 11124–11134.
[20] W. Jia, B. Jia, F. Qu, et al., Dalton Trans. 42 (2013) 14178–14187.
[21] X. Gao, J. Wang, J. Yu, et al., CrystEngComm 17 (2015) 6328–6337.